LATTICE-BOLTZMANN SCHEME FOR DENDRITIC GROWTH IN PRESENCE OF CONVECTION

Dmitry Medvedev, Klaus Kassner

Institute of Theoretical Physics,
Otto-von-Guericke-University, Universitätsplatz 2,
39106 Magdeburg, Germany
e-mail: *dmedv@physik.uni-magdeburg.de*

Magdeburg
2004

SUMMARY

A combined phase-field/lattice-Boltzmann scheme is proposed to simulate dendritic growth from supercooled melt, with account for flows of liquid and thermal convection.

MODEL

1. Simulation of solidification — phase-field model (Karma and Rappel, 1996).
2. Flow of liquid — lattice-Boltzmann-BGK (LBGK) method with incorporated interactions with solid and thermal convection. This step can be left out in the case of purely diffusional growth.
3. Conductive and convective heat transfer — multicomponent LBGK method.

Phase-field model

$$\tau(\theta)\phi_t = (2\phi - 1 - 4\lambda\overline{T}\,\phi(1-\phi))2\phi(1-\phi) + \nabla\cdot\left(W^2(\theta)\nabla\phi\right) - \partial_x\left(W(\theta)W'(\theta)\phi_y\right) + \partial_y\left(W(\theta)W'(\theta)\phi_x\right),$$

$$\overline{T}_t + \mathbf{U}\nabla\overline{T} = D\nabla^2\overline{T} + \phi_t.$$

ϕ — concentration of solid phase ($0 \le \phi \le 1$),
$\overline{T} = \rho c_p(T - T_m)/L$ — normalized temperature,
W — anisotropic interface width,
τ — relaxation time.
In order to obtain zero kinetic coefficient, the following relations must be imposed

$$W = W_0 A(\theta),\ \tau = \tau_0 A^2(\theta),\ \lambda = \frac{2ID\tau_0}{(K+JF)W_0^2}.$$

Anisotropy function

$$A(\theta) = 1 + \varepsilon\cos 4\theta,$$

$\theta = \arctan(\phi_y/\phi_x)$ — the angle between the local interface normal and the X axis. We assume $\tau_0 = 1$, $W_0 = 1$.
Interface stiffness $\alpha = 15\varepsilon$.

This equation was discretized on a uniform spatial lattice with a step $\Delta x = 0.4$, and solved using the explicit Euler method with time step Δt.

Lattice-Boltzmann method

- Regular lattice, lattice vectors $\mathbf{e}_k$
- Discrete set of velocities $\mathbf{c}_k \Delta t_{LB} = \mathbf{e}_k$

Variables f_k — one-particle distribution functions.
Evolution equation

$$f_k(t, \mathbf{x}) = f_k(t - \Delta t_{LB}, \mathbf{x} - \mathbf{c}_k \Delta t_{LB}) + \frac{f_k^{eq} - f_k}{\tau_f}.$$

Propagation and collisions, τ_f — Maxwellian relaxation time. Later on $\Delta t_{LB} = 1$.
Kinematic viscosity $\nu = (\tau_f - 1/2)/3$.
Hydrodynamic quantities

$$\rho = \sum_k f_k, \qquad \rho \mathbf{U} = \sum_k f_k \mathbf{c}_k.$$

Equilibrium distribution functions $f_k^{eq}(\rho, \mathbf{U})$.
Interaction with solid

$$\mathbf{F}_d = -\nu \frac{2h\phi^2}{W_0^2} \mathbf{U}.$$

Thermal convection — buoyancy force

$$\mathbf{F}_c = -\rho\alpha(1 - \phi)(\overline{T} - \overline{T}_0)\mathbf{g},$$

α — coefficient of thermal expansion, $\mathbf{g}$ — gravity acceleration.

Heat transport

Second set of distribution functions N_k.
Evolution equation

$$N_k(t+\Delta t, \mathbf{x}+\mathbf{c}_k\Delta t) = N_k(t,\mathbf{x}) + \frac{N_k^{eq} - N_k}{\tau_T}.$$

$$N_k^{eq} = N_k^{eq}(\overline{T}, \mathbf{U} + \Delta\mathbf{U}/2)$$

$$\overline{T} = \sum_k N_k, \quad \mathbf{U} = \sum_k f_k \mathbf{c}_k / \sum_k f_k, \quad \Delta\mathbf{U} = \mathbf{F}/\sum_k f_k$$

$\mathbf{F} = \mathbf{F}_d + \mathbf{F}_c$ — total force.
Resulting equation

$$\frac{\partial \overline{T}}{\partial t} = \mathbf{U}\nabla\overline{T} + \chi\nabla^2\overline{T} + \frac{\partial\phi}{\partial t}.$$

Thermal diffusivity $\chi = (\tau_T - 1/2)/3$ everywhere (symmetric model).

Shear flow

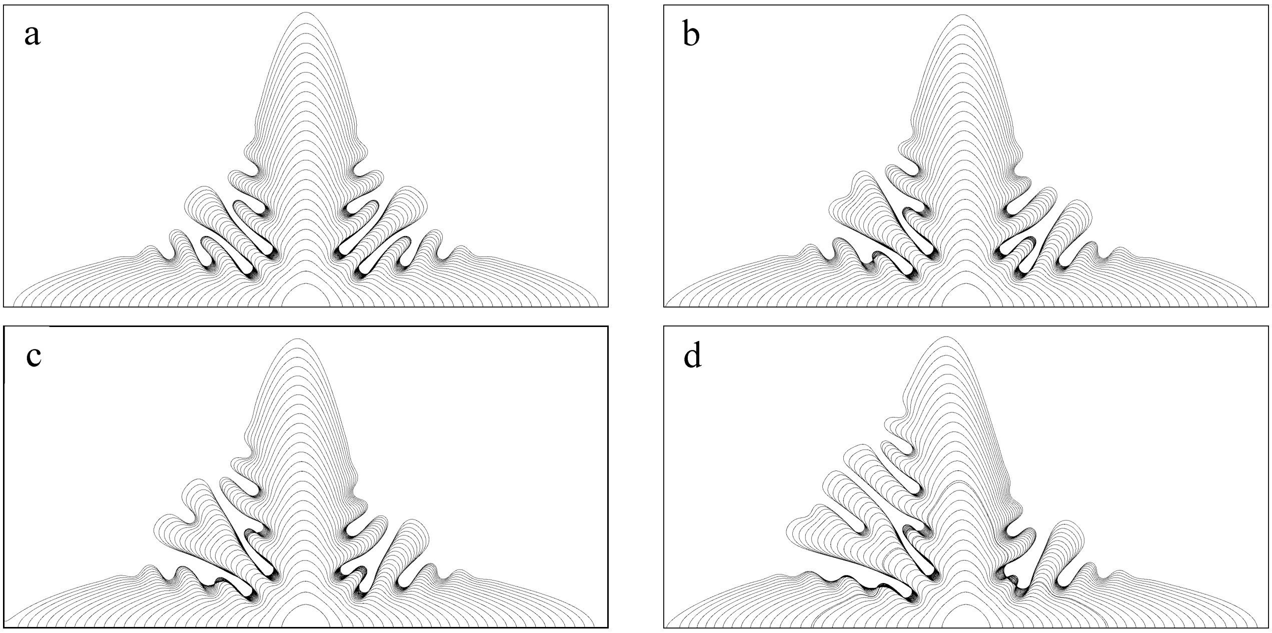

Figure 1: Dendrite. $\Delta = 0.7, 15\varepsilon = 0.15$. Reduced velocity $\overline{U}$=0 (a), $\overline{U}$=0.0123 (b), $\overline{U}$=0.0247 (c), $\overline{U}$=0.0493 (d). Interface contours are shown at time increments of 50

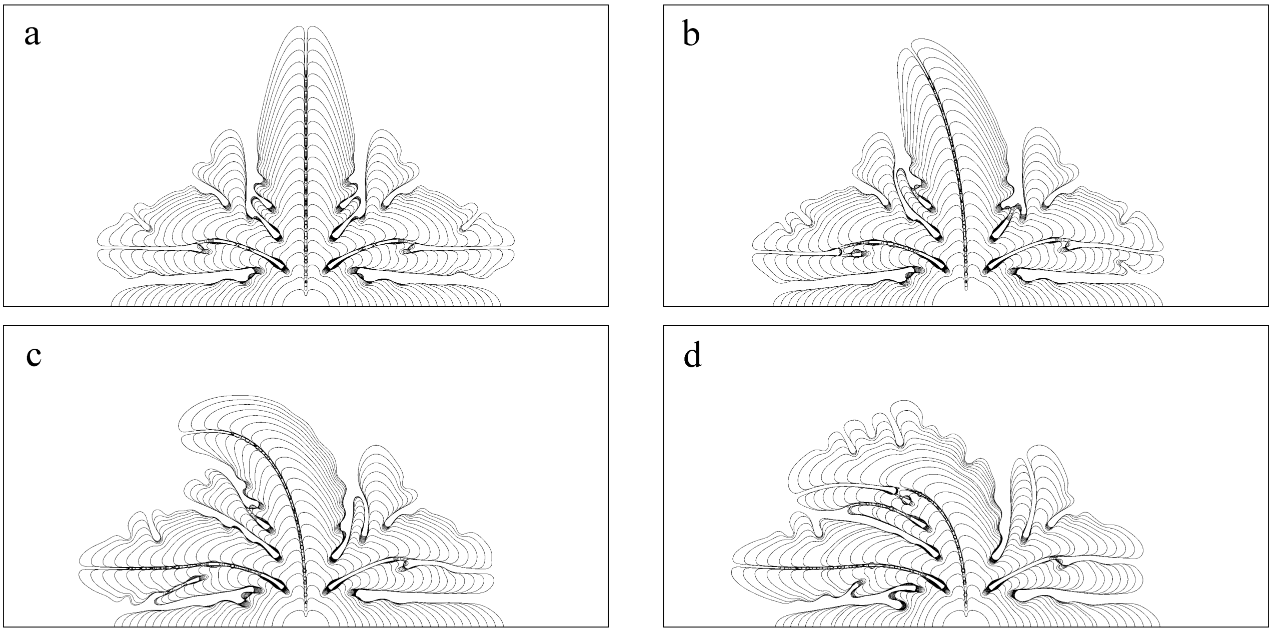

Figure 2: Seaweed. $\Delta = 0.8, 15\varepsilon = 0.15$. Reduced velocity $\overline{U}$=0 (a), $\overline{U}$=0.0247 (b), $\overline{U}$=0.0493 (c), $\overline{U}$=0.0987 (d). Interface contours are shown at time increments of 20

Thermal convection

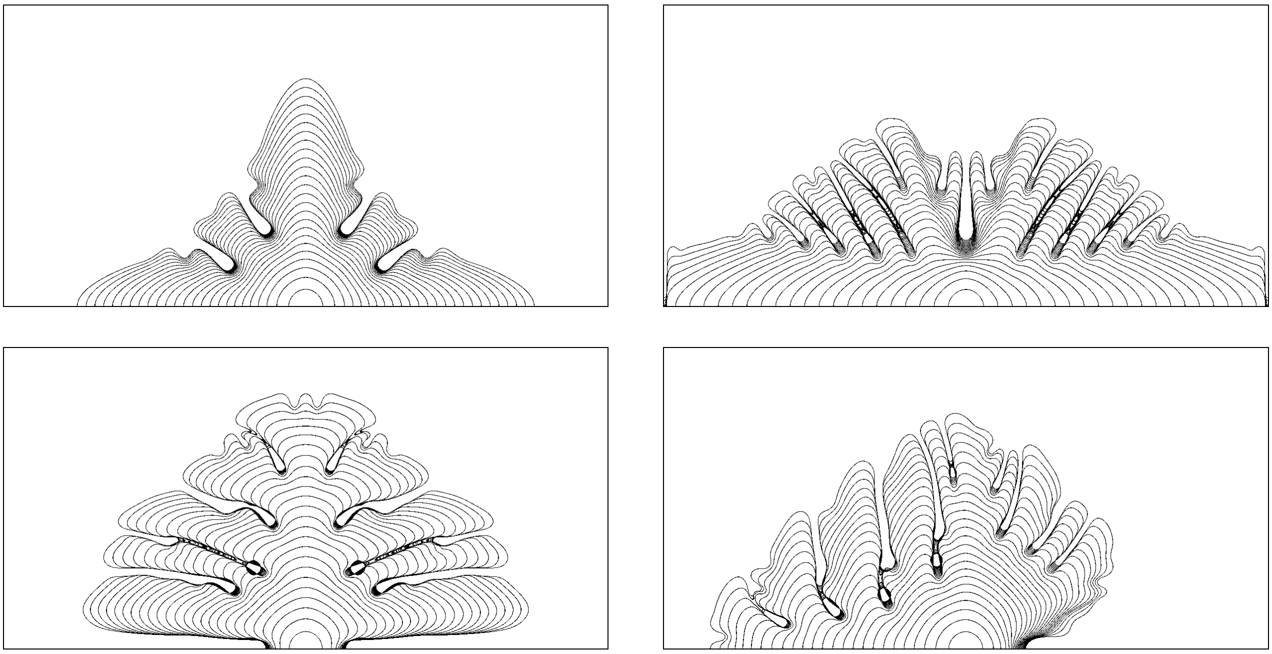

Figure 3: Dendritic growth with convection. $\Delta = 0.8, 15\varepsilon = 0.3$. $\beta g_y = 0.0$, $g_x = 0$ (a); $\beta g_y = -0.0005$, $g_x = 0$ (b); $\beta g_y = 0.0005$, $g_x = 0$ (c) and $g_y = 0$, $\beta g_x = 0.0005$ (d). Interface contours are shown at time increments of 10

Influence of parallel flow on the growth

Growth of the dendrite tip in the parallel flow

$\Delta = 0.65, 15\varepsilon = 0.75$, grid size 300×600

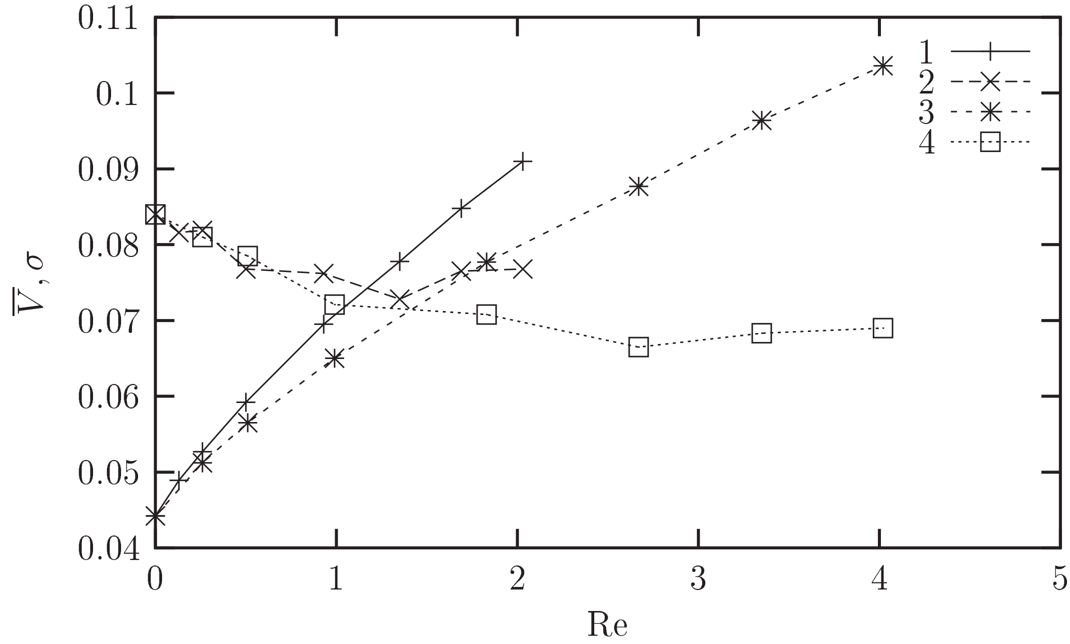

Figure 4: Dependence of reduced velocity $\overline{V}$ and selection parameter σ on flow Reynolds number. 1 — $\overline{V}, \nu = 1/3$; 2 — $\sigma, \nu = 1/3$; 3 — $\overline{V}, \nu = 1/6$; 4 — $\sigma, \nu = 1/6$

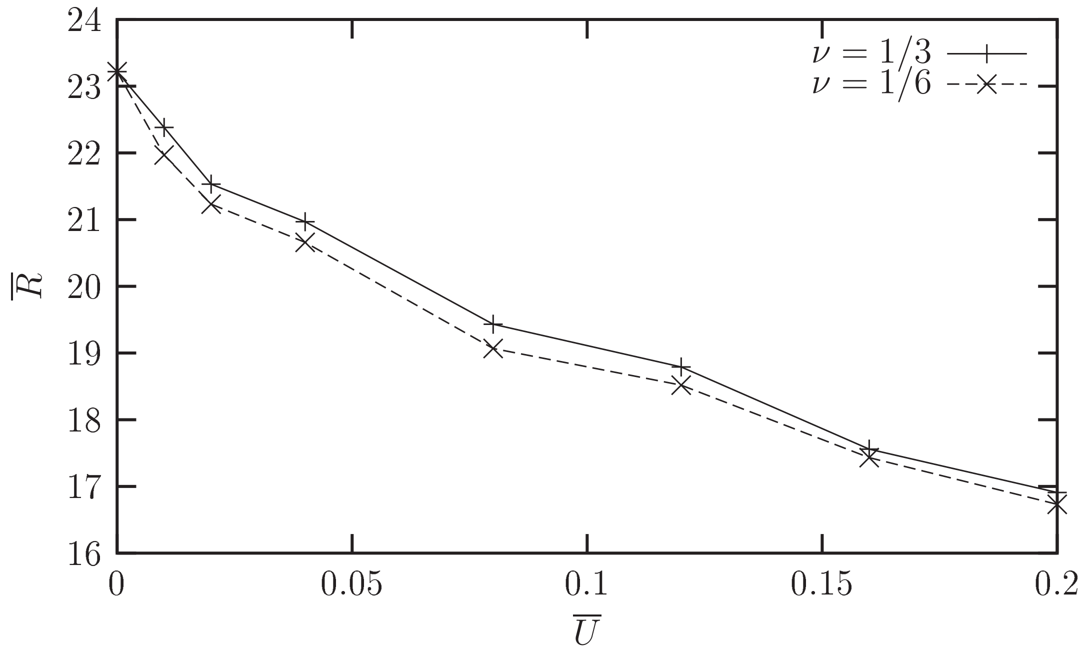

Figure 5: Dependence of reduced tip radius $\overline{\rho}$ on reduced flow velocity $\overline{U}$

Growth of the dendrite tip in the parallel flow

$\Delta = 0.45, 15\varepsilon = 0.75$, **grid size 400×800**

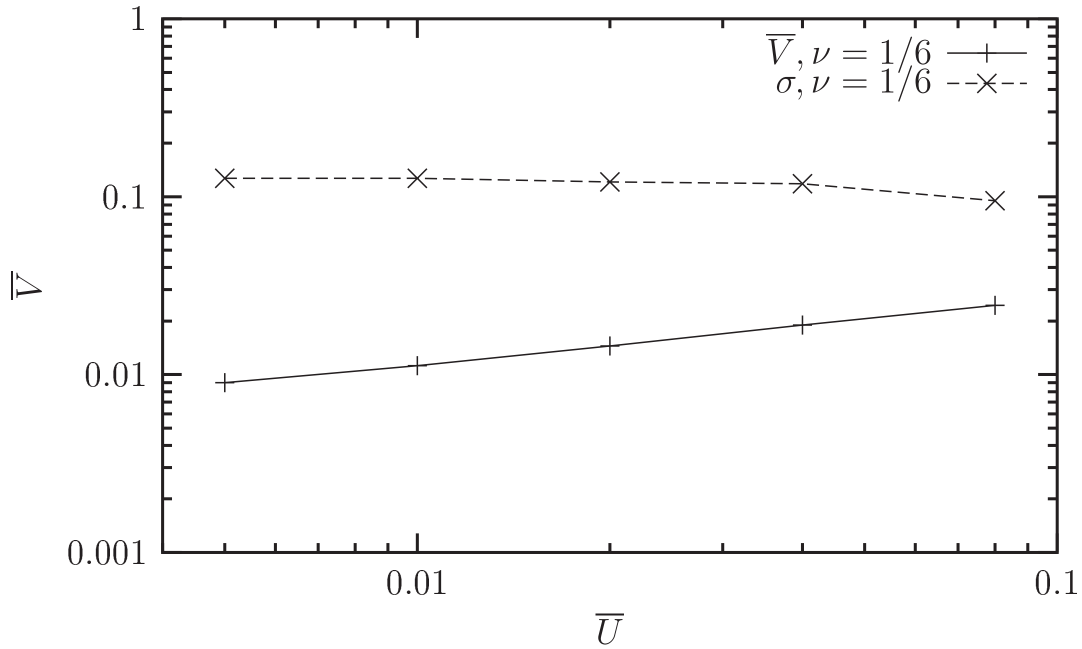

Figure 6: Dependence of reduced velocity $\overline{V}$ and selection parameter σ on reduced flow velocity $\overline{U}$

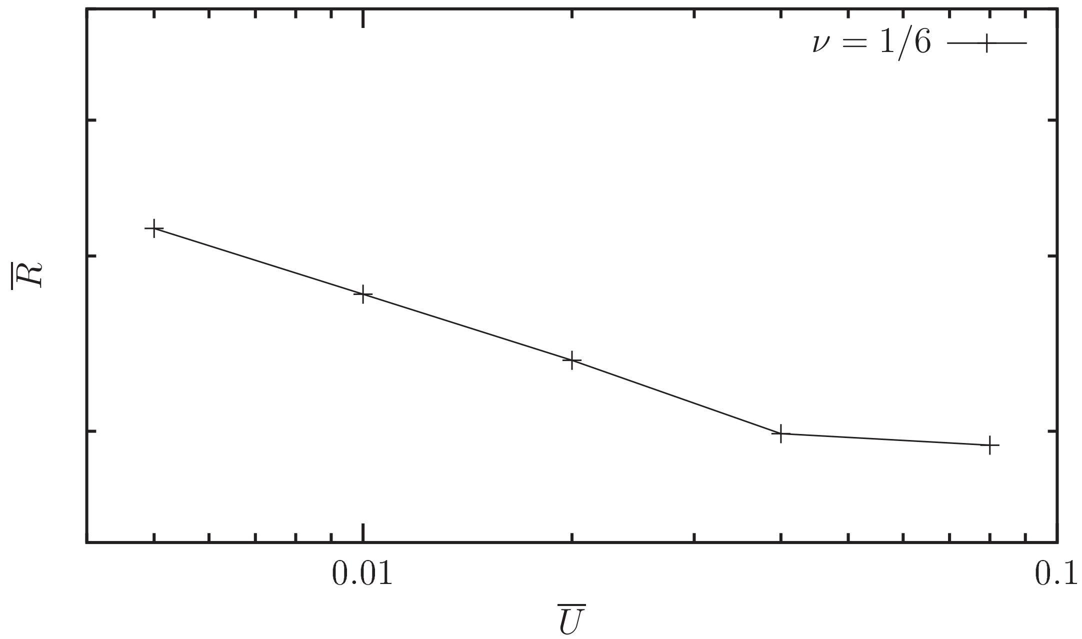

Figure 7: Dependence of reduced tip radius $\overline{\rho}$ on reduced flow velocity $\overline{U}$

Dependences $\overline{V} \sim \overline{U}^{0.38}, \quad \overline{R} \sim \overline{U}^{-0.16}, \quad \sigma \sim \overline{U}^{-0.04}$

Growth of the dendrite tip in the parallel flow

$\Delta = 0.7, 15\varepsilon = 0.15$, grid size 400×800

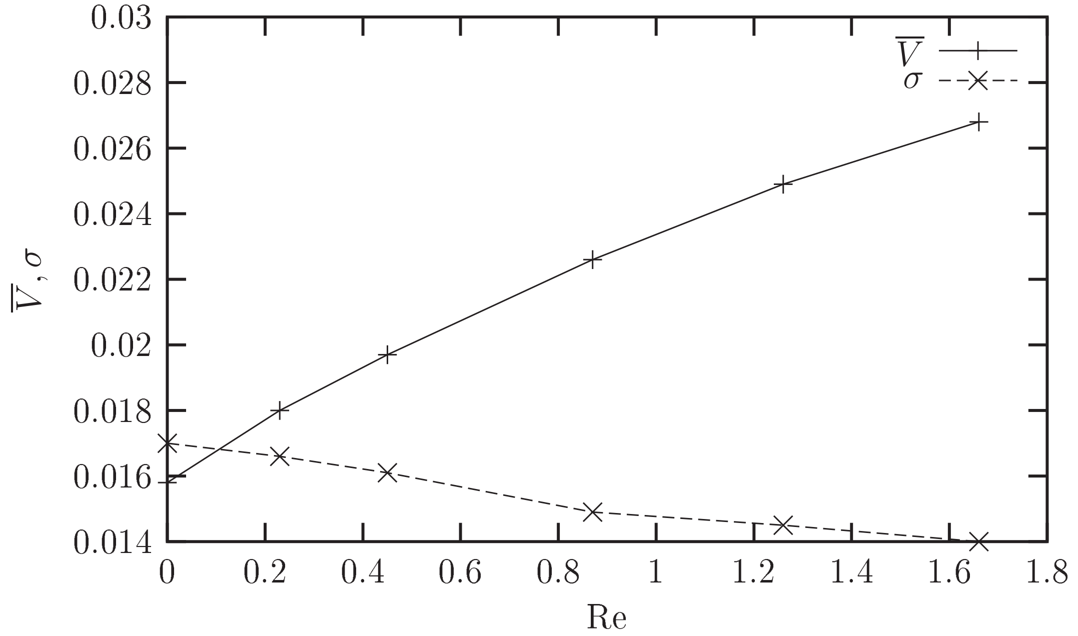

Figure 8: Dependence of reduced velocity $\overline{V}$ and selection parameter σ on flow Reynolds number

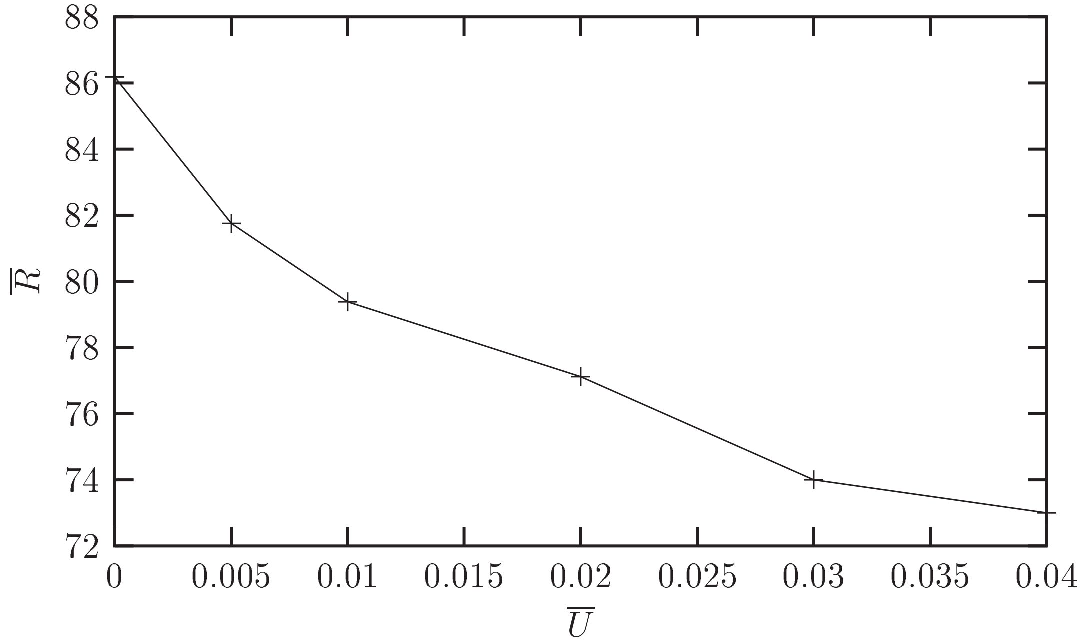

Figure 9: Dependence of reduced tip radius $\overline{\rho}$ on reduced flow velocity $\overline{U}$

Sidebranching in the parallel flow

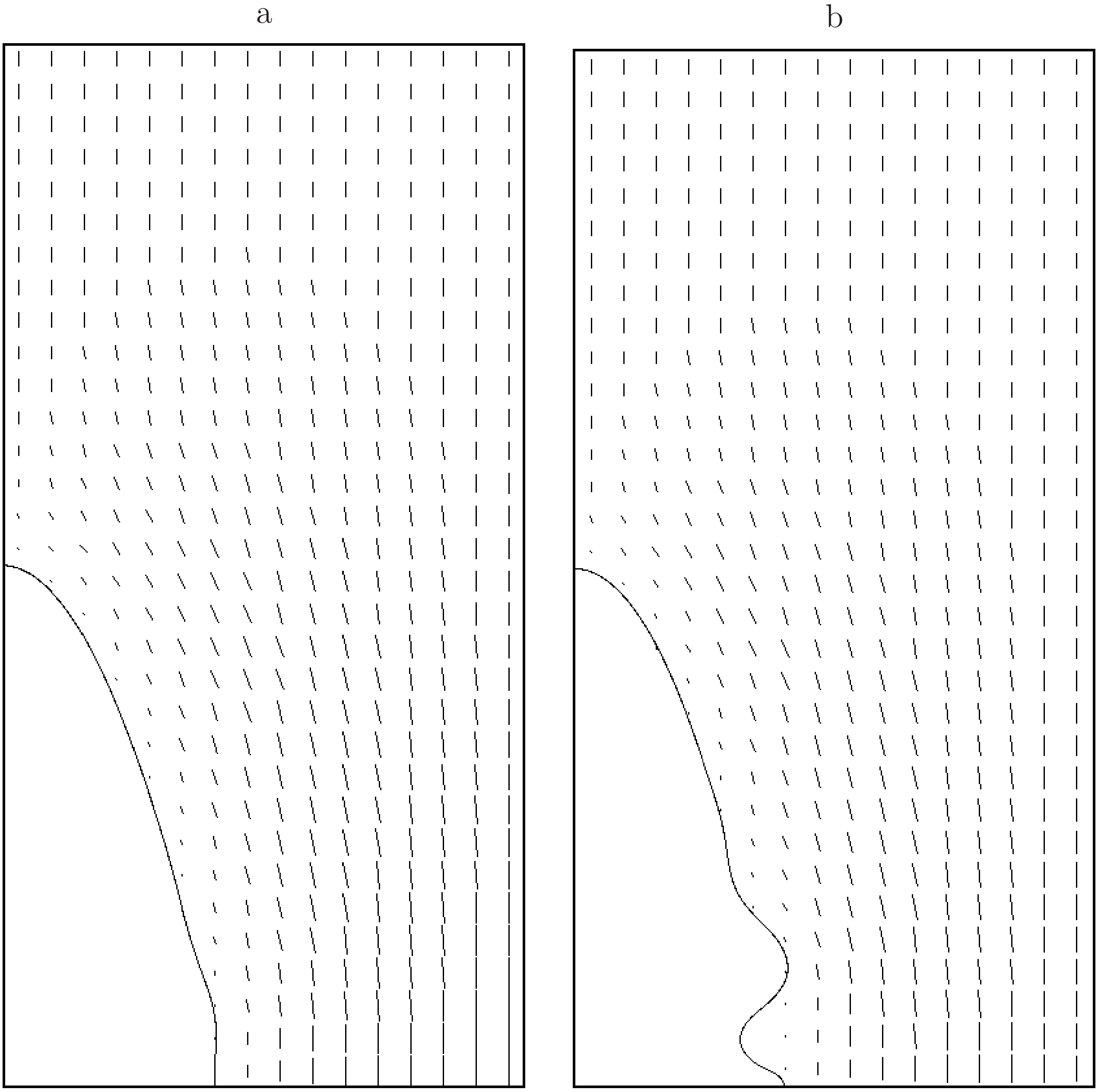

Figure 10: Growth of side branches, $\Delta = 0.7, 15\varepsilon = 0.15$. Reduced flow velocity $\overline{U} = 0.01$ (a) and $\overline{U} = 0.04$ (b)

At large flow velocities, oscillations of tip velocity were observed, accompanied by the enhanced growth of side branches.

Conclusions

The main results are

- Simulations showed strong influence of external shear flow on the seaweed growth (Fig. 2)
- Influence of parallel flow on the operation state of dendrite tip was investigated quantitatively (Fig. 4–9)
- Simulations demonstrated onset of velocity oscillations and enhancement of sidebranching under parallel flow (Fig. 10)